Ocular Dominance and Functional Asymmetry in Visual Attention Networks

Sinan Liu,[1] Bingyang Zhao,[1] Chaoqun Shi,[1] Xuying Ma,[1] Bernhard A. Sabel,[2] Xiping Chen,[1] and Luyang Tao[1]

[1]Department of Forensic Science, Soochow University, Suzhou, China
[2]Institute of Medical Psychology, Otto-von-Guericke University Magdeburg, Leipziger Strasse 44, 39120 Magdeburg, Germany

Correspondence: Xiping Chen and Luyang Tao, Department of Forensic Science, Soochow University, 215021 Suzhou, China; xipingchen@suda.edu.cn; taoluyang@suda.edu.cn.

SL and BZ equal contributions to the manuscript.

Received: November 15, 2020
Accepted: March 15, 2021
Published: April 7, 2021

Citation: Liu S, Zhao B, Shi C, et al. Ocular dominance and functional asymmetry in visual attention networks. *Invest Ophthalmol Vis Sci.* 2021;62(4):9. https://doi.org/10.1167/iovs.62.4.9

Purpose. The dorsal attention network (DAN) and the ventral attention network (VAN) are known to support visual attention, but the influences of ocular dominance on the attention networks are unclear. We aimed to explore how visual cortical asymmetry of the attention networks correlate with neurophysiological oscillation and connectivity markers of attentional processes.

Methods. An oddball task with concentric circle stimuli of three different sizes (i.e., spot size of 5°, 20°, or 30° of visual angle) was used to vary task difficulty. Event-related oscillations and interareal communication were tested with an electroencephalogram-based visual evoked components as a function of ocular dominance in 30 healthy subjects.

Results. Accuracy rates were higher in the dominant eyes compared with the nondominant eyes. Compared with the nondominant eyes, the dominant eyes had higher theta, low-alpha, and low-beta powers and lower high-alpha powers within the nodes of VAN and DAN. Furthermore, visual information processed by the dominant and nondominant eye had different fates, that is, the dominant eyes mainly relied on theta and low-alpha connectivity within both the VAN and the DAN, whereas the nondominant eyes mainly relied on theta connectivity within the VAN and high-alpha connectivity within the DAN. The difference in accuracy rate between the two eyes was correlated with the low-alpha oscillations in the anterior DAN area and low-alpha connectivity of the left DAN.

Conclusions. The ocular dominance processing and interareal communication reveal a cortical asymmetry underlying attention, and this reflects a two-way modulatory mechanism within attention networks in the human brain.

Keywords: attention networks, ocular dominance, visual cortical asymmetry, event-related oscillations, interareal communication

The ability to rapidly detect and direct attention towards significant changes in the visual environment is essential for survival. One of the most widely used experimental paradigms to investigate this ability is commonly called the "oddball" task, which probes salience detection and the engagement of attention.[1] Targets embedded in a stream of standards produce distinct responses that can be recorded noninvasively with electroencephalogram (EEG). Habituation for the standards, one of the primary universal learning mechanisms, can be defined simply as the decrement in response to repeated stimuli. In addition, habituation can help individuals to focus on important stimuli for salience detection and, thus, can be viewed as an integral part of attention detection.[2] The brain mechanisms underlying this attentional process are supported by the activation of two brain functional networks: the dorsal attention network (DAN) and the ventral attention network (VAN).[3] On one hand, the increased EEG theta activities represent the typical recruitment of DAN and VAN during the attention-related target processing.[4] The increased beta-band power represents the intention of the maintenance of the current cognitive state.[5] On the other hand, two-way interactions of the DAN and VAN alpha rhythm were observed during the process of attention. The decreased activity in the alpha band may signify a state of enhanced excitability of the visual system to improve the processing of the forthcoming stimulus.[6,7] In contrast, the increased alpha activity may act as a neural signature of the attentional process to suppress task-irrelevant information from sensory inputs when irrelevant distractors as demonstrated in an audiovisual paradigm.[8] In addition, the mu rhythm—a fulcrum for transitional brain states—is a field oscillation around 10 Hz,[9] and mu power decreases with increased attention, which is consistent with a state of enhanced excitability in alpha activity.[10] Although these studies shed light on the physiological basis of attention, these experiments were all conducted under binocular viewing conditions. They did not consider possible influences of ocular dominance which plays a recognized and important role in normal and abnormal vision. Therefore, there is a need to

clarify the role of eye dominance in visual attention network processing.

Eye dominance can be determined by three criteria: acuity, sensation, or sighting.[11] In observers completely blind in one eye or those with extreme amblyopia, the intact eye will be dominant, fulfilling all three criteria because it is used for acuity, sensory perception, or sighting. In contrast, eye dominance in normal observers is defined (or fulfilled) by only one criterion, which may lead to different results compared with cases, where all three criteria are fulfilled. Thus, a single unitary concept of eye dominance could not yet be established.[12] "Acuity dominance" refers to the eye with better visual acuity, a key function of vision in patients with ocular diseases. "Sensory eye dominance" is usually established by having the observer view a binocular rivalry target, which cannot be performed monocularly. It relies on the neural mechanisms underlying the excitatory-and-inhibitory balance between binocular viewing.[13] Finally, "sighting eye dominance" is reliable within a given test, because it is based on an either/or judgement as to which eye is preferably used for monocular viewing. With both eyes open, people with normal binocular vision have no sense that one eye contributes more than the other to the combined binocular view.[14] Therefore, to study the processing mechanism of eye dominance, we now use monocular tasks to measure sighting eye dominance.

There are some differences between a dominant and a nondominant eye both in structure and visual processing aspects. For example, ocular dominance was associated with structural differences in the retina, such as retinal nerve fiber layer thickness or the ganglion cell–inner plexiform layer thickness profile in the macula.[15] According to the anatomic arrangement of the human visual system, the optic nerve pathway is different between binocular eyes, especially in the part of the central visual pathway which is located behind the optic chiasm.[16] Indeed, both the structural magnetic resonance imaging and the functional magnetic resonance imaging studies found that the ocular dominance was related with the structural asymmetry and the response differences in cortical visual areas.[17,18] Behavioral and physiological studies demonstrated that participants have significantly faster reaction times (RTs), better accommodative function and shorter response latency of steady-state visually evoked potentials when using their dominant eyes.[19–21] Although the relationship between ocular dominance and the visual cortex is well-recognized, the influence of ocular dominance on visual attention networks is unknown. Specifically, the frequency-specific brain oscillations and precise network processing mechanisms of this ocular asymmetry have not been well-studied. Therefore, because behavioral performance of the dominant eye is greater than that of the nondominant eye, we hypothesized that ocular dominance may activate different cortical regions and their networks of attention and hence determine the strength of attention network activation. This differential network activation, in turn, is supported by associated physiological differences in power and functional connections in the theta, alpha, and beta band. In other words, visual processing by the dominant and the nondominant eye might recruit different underlying visual attentional mechanisms of DAN or VAN during salience detection, and this, in turn, may relate to task difficulty.

In the present study, we therefore explored the functional asymmetry of attention networks between the dominant and nondominant eye during visual attentional information processing. Based on our previous study,[22] we designed a three-stimulus oddball paradigm presenting visual stimuli of different visual field sizes (5°, 20°, and 30° visual angles) to the dominant versus nondominant eye of normal subjects. The central retinal sector has the highest resolution and its projections, occupying more than one-half of the visual cortex, which can be described on the basis of the so-called magnification factor.[23] In this manner, we were able to vary task difficulty of attention within the 30° central visual field boundary[24,25] with the smaller targets considered to be easier.

Using time–frequency EEG analyses and interareal communication, we now describe how ocular dominance influences the underlying neural activity of the attention networks in the theta, alpha and beta sub-bands, respectively. Ocular dominance and stimulus sizes comprised the independent variables, and then we measured outcome changes in the EEG (dependent variables). We expected that no matter what the stimulus size would be, the target superiority would be reflected in event-related oscillation activities. Specifically, we predicted that behavioral performance, event-related oscillations, and functional connectivity decreased with increasing task difficulty. As we now show, the dominant eye and nondominant eye are involved in different attention networks during salience detection and in the engagement of attention, yet they cooperate to process complex visual tasks.

Methods

Participants

Sixty eyes were sampled randomly from 30 healthy students balanced for sex (age = 20–27 years, M = 23.4 years, standard deviation [SD] = 1.238; right handed). All subjects from Soochow University volunteered to participate in the experiment and gave their written consent as approved by the Soochow University ethics committee. The study protocol was approved by the Ethics Committee of Soochow University (reference number: SZUM2008031233) and was carried out in accordance with the Declaration of Helsinki. All participants had normal or corrected-to-normal vision as per routine visual acuity test and no history of neurological or psychiatric disorders. Ocular dominance was determined with the hole-in-card test.[26] Subjects were instructed to fixate an object in the room with both eyes open through a "hole" formed by their hands having their arms stretched to ensure that the hole is in the middle line of the subjects' body. Then they were asked to alternately close the right or the left eye and report when the target was visible. The dominant eye was defined as being the one that could maintain the fixed object centered in the hole or the one that caused greater change when closed. In addition, a modified Porta test[27] was used as a proper control. Subjects were instructed to stretch one arm with the index finger pointed up and look at the line formed by the index finger with an object in the room with both eyes open. Then they were told to alternately close the right and the left eyes and report if the finger moved. The eye that was open with the finger that moved the least is the dominant eye. Only the consistent results provided by the two tests would be included in our study. Therefore, there were 30 eyes balanced for left or right sidedness and sex (15 right eyes, 15 males) in the dominant eye condition, and other 30 eyes balanced for left/right sidedness and sex (15 right eyes, 17 males) in the nondominant eye condition.

Investigative Ophthalmology & Visual Science

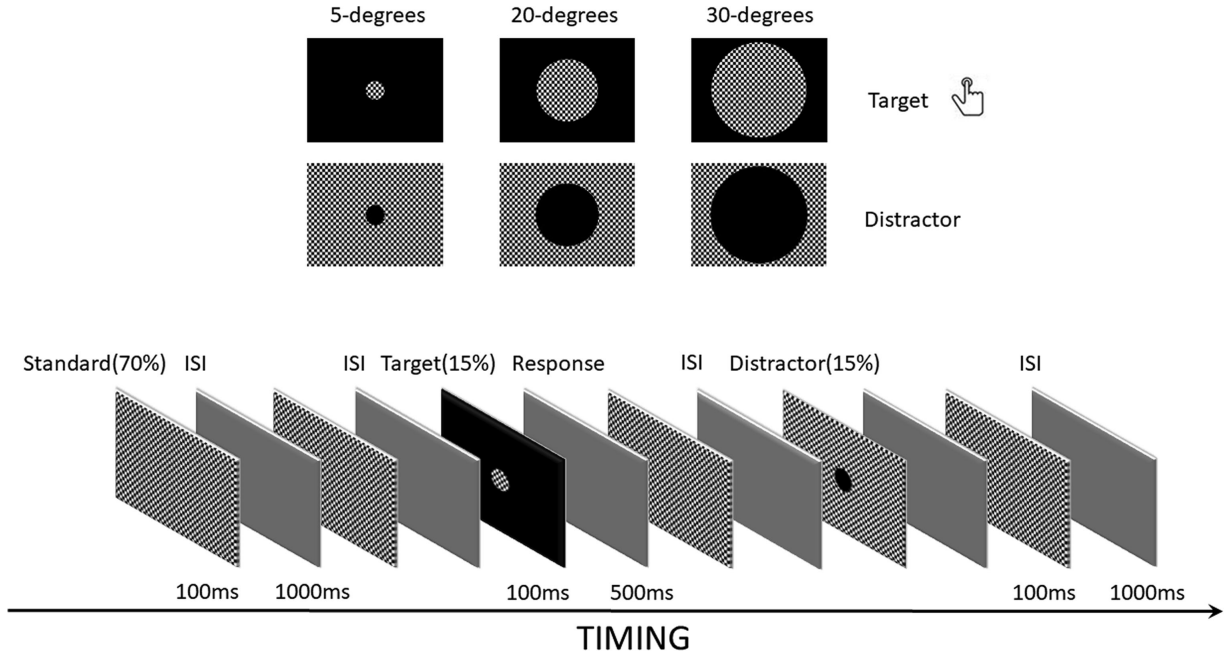

Figure 1. Overview of the three-stimulus oddball paradigms task stimulus categories and trial sequences. There were the standard (70%), target (15%), and distractor (15%) trials in the experiment. A stimulus was presented (100 ms) consisting of the center disc varied with stimulus size conditions. Stimuli were interspersed with an interval (1000 ms) and the response window was 500 ms. The three possible targets showing in the top row, linked to only one response, which was press a button with right index finger as quickly as possible. And the distractor stimulus can be seen in the second row, with no button press to be performed.

There was no significant gender difference between the two ocular dominance conditions ($\chi^2_{0.05,1} = 0.268$; $P = 0.605$).

Experimental Design

Stimuli. A visual oddball paradigm with three stimuli was used which was repeated for each of the stimulus size conditions (central 5°, 20°, or 30° of the visual field). Here, smaller stimuli were considered to be easier because the attentional spotlight was more focused, and our behavioral results supported this assumption. Each stimulus size condition included a four-block design with 200 stimuli presented in each block, including frequent standard stimuli (black and white checkerboard), infrequent target stimuli (round central checkerboard and surrounding the black area), and distractor stimuli (round central black disc and surrounding the checkerboard). The probability of standard stimuli, target stimuli, and distractor stimuli was 70%, 15%, and 15%, respectively (Fig. 1). All stimuli were displayed on a 17-inch Dell CRT monitor with a light gray background via E-prime software. The size of the presentation slides was the same as the size of the monitor. The unit element of the checkerboard displayed a $32' \times 32'$ visual angle, and the visual angle of central round checkerboard or black disc varied in sizes of 5°, 20°, and 30° stimuli. The frame of the computer monitor was covered with black cardboard, so that the reaction of the participants to the distinguishable stimulus sizes could not be influenced by the other physical parameter but by the stimulus pictures only. The stimulus presentation time was 100 ms and the interstimulus interval was set at 1000 ms, including a 500-ms response window. To ensure the effectiveness of the oddball paradigm and avoid habitual responses, the order of stimuli was pseudorandom in each block. In this way, two target or distractor stimuli were not displayed continuously with at least two frequent standard stimuli between them. After an initial practice session, the total number of 2400 trails (12 blocks) were presented to each eye (see Fig. 1). The order of the stimulus presentation to the dominant or nondominant eye was counterbalanced across subjects.

Procedure. Participants sat at a distance of 40 cm away from the screen in a dimly lit and soundproof chamber using an eye patch for monocular viewing. Subjects were instructed to keep their eye focused on the center fixation cross of the screen and they were asked to avoid eye blinks and unnecessary body movements. The stimulus pictures were displayed on the screen semirandomly with the visual stimuli which varied in sizes (central 5°, 20°, to 30°). The task was to press a button on a standard USB keyboard with the index finger of the right hand (all subjects are right handed) as fast as possible when a target stimulus was presented but to ignore all other stimuli. We recorded the RT and accuracy rate. To avoid eye strain, a short break was provided after completing each block.

Data Acquisition and Analysis

EEG Data Acquisition. A continuous EEG was recorded with a NeuroScan 4.3 Amplifier. The 32-channel Ag/AgCl electrodes were placed on the scalp with an elastic head cap according to the extended 10–20 system. The signals were referenced to the root of nose, with a ground channel at FPZ. Eye movements were recorded with four additional electrodes, and two of them were placed 0.5 cm lateral from the outer canthi of each eye to record the horizontal electro-oculogram. The vertical electro-oculogram was recorded with two electrodes above and below the axis of the left eye. The impedance between scalp and electrode

Investigative Ophthalmology & Visual Science

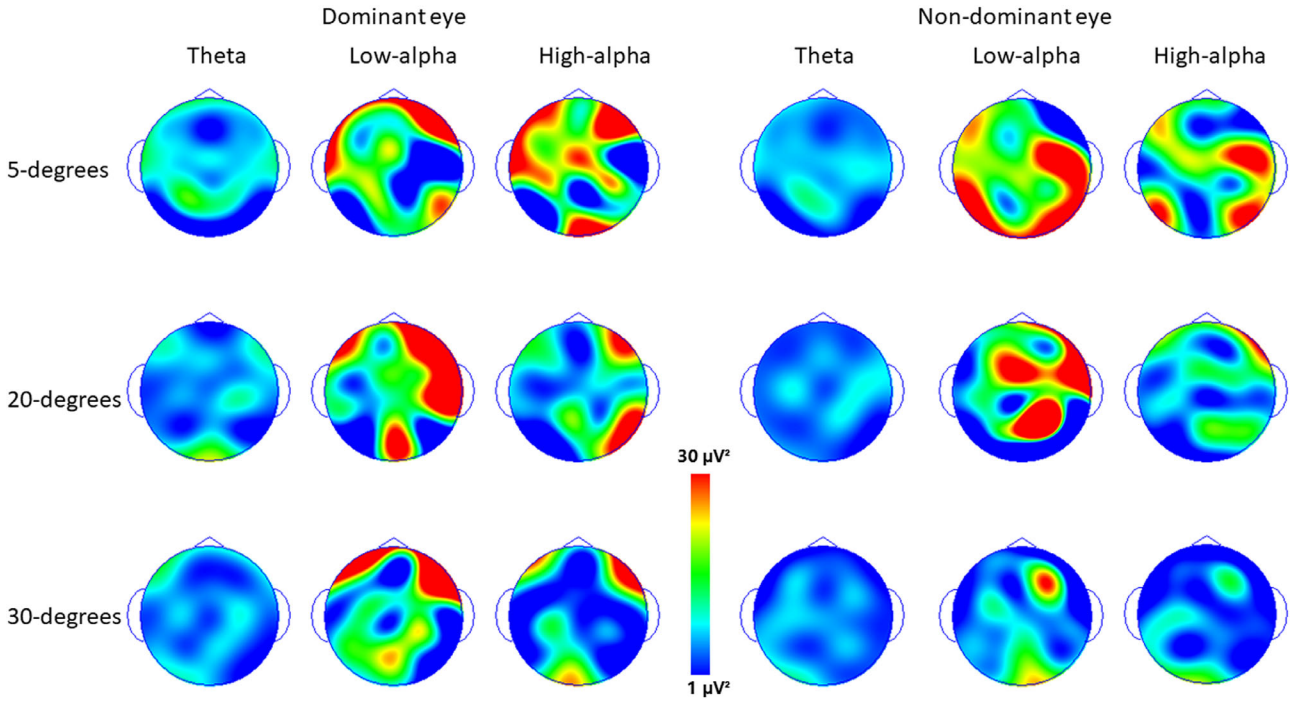

Figure 2. Topographic plots. Topography of theta, low-alpha and high-alpha power separately plotted for dominant eye (left panel) and nondominant eye (right panel) averaged across all trials within 5° (top panel), 20° (median panel) and 30° stimuli (bottom panel) blocks.

was maintained always below 5 kΩ and data were recorded at 1000 Hz (resolution: 32 bits; 0.1 Hz high and 100 Hz low pass online filters).

Time–Frequency Analyses. The oscillatory activities in the standard and target stimulus condition were analyzed among the three stimulus sizes by EMSE 5.6 software (Source Signal Imaging, San Diego, CA). EEG data were re-referenced to the common average reference of all electrodes. An electro-oculogram artifact correction was conducted to remove eyeblinks or saccades. The corrected EEG was segmented for an epoch with 500 ms before the stimulus and 550 ms after the stimulus. Artifacts exceeding ±100 μV were rejected from analyses. Then, the surface Laplacian transformation was used to decrease the volume conduction from the distal sites and increase sensitivity to radial sources directly underlying each electrode.[28] The powers of these frequency bands were computed by continuous Morlet wavelet transform with three cycles, which was an original arithmetic of the software and calibrated to cover the entire frequency band of interest. The Morlet wavelet consists of a complex exponential function localized in time by a Gaussian envelope. The initial spread of the Gaussian wavelet was set to $2.5/\pi\omega 0$ ($\omega 0$ being the central frequency of the wavelet).[29] To explore the underlying neural activity of the attention networks, the frequency bands of interest were theta (4–7 Hz), low (8–10 Hz), and high-alpha (10–12 Hz) as well as low-beta (13–20 Hz) and high-beta (20–30 Hz).[30–32] Event-related oscillations were broadly categorized into either evoked (phase locked) or induced (non–phase locked). And the combination of both evoked and induced oscillatory power was named as the total power.[33]

According to the grand averaged spectrum, before dividing into the different conditions, we picked times of interest based on the combined data so as not to provide a biased time window selection: the total power and the induced power of theta band were measured from 50 to 300 ms after the stimuli and the alpha and beta band were measured in the range of 150 to 400 ms after the stimuli. The phase-locked power of the theta, alpha, and low-beta bands was measured in the range of 50 to 250 ms after the stimuli, whereas the high-beta band was measured in the range of 50 to 200 ms after the stimuli. After normalizing the baseline, the mean value at each frequency band was automatically calculated for the specified intervals in each channel.

Numerous studies demonstrated that the frontal eye fields and the superior parietal lobules support the DAN, whereas the right-lateralized VAN involves the ventral frontal cortex and the temporoparietal junction.[3] Also, the previous study of attention network defined regions of interest (ROIs) based on brain atlas.[34] Our topographic plots (Fig. 2) showed the theta power to be focused on the parietal areas, whereas the low-alpha and high-alpha power were dispersed and divided into anterior and posterior areas, mainly closer to the frontal and temporal areas. Based on the anatomic Brodmann atlas,[35] we combined the known EEG functional approaches to reveal the relationship between the location of an electrode and the underlying area of cerebral cortex.[36] For our topographic plots, we chose the frontal area (F3/4, FC3/4), the parietal area (CP3/4, P3/4), the ventral frontal area (F7/8, FT7/8), and the temporal area (T3/4, T5/6) as ROIs for further analysis, which defined these brain areas as the DAN anterior area, the DAN posterior area, the VAN anterior area, and the VAN posterior area, respectively.

Estimation of the Phase-Locking Value (PLV). All analyses were completed using MATLAB R2014a with the EEGLAB toolboxes,[37] as well as custom scripts. The channel location file was mapped into the data. Then, the EEG data were re-referenced offline to the average reference. For the subsequent analysis, the re-referenced EEG were segmented into 1050-ms epochs from –500 ms to 550 ms relative to the

Investigative Ophthalmology & Visual Science

onset of stimuli, including a baseline period of –500 ms to –200 ms. The average voltage of this baseline before the target was subtracted on each trial for every electrode. Trials with a wrong reaction or omission were not included in any analysis. Then, the surface Laplacian transformation were used to reduce volume conduction from distal sites. Although not a source localization analysis, Laplacian renders the electrodes maximally sensitive to radial sources directly underlying each electrode,[38] so the EEG signal on sensor level can be regarded as indices of the activation of the underlying brain structure. The PLV over trials between pairs of electrodes was computed with custom scripts as a measure of functional connectivity to discuss the synchronization of the neural responses across channels.[39] The frequency band activity was obtained from FIR filtering procedure. The instantaneous phase information was computed from the Hilbert transform of the signal, and the PLV is given by

$$PLV(t,f) = \frac{1}{N}\left|\sum_{n=1}^{N} e^{i(\Phi_{n,x}(t,f)-\Phi_{n,y}(t,f))}\right|$$

for each time bin t, frequency band f, trial n, and pair of electrodes.[40]

As a normalized measure of temporal synchronization, an increase in the PLV (scale from 0 to 1) can be defined as an enhancement of functional connectivity between pairs of EEG channels in a given frequency band, but it can't confirm the direction and the property of information flow.[41] According to prior attention networks studies and the intrahemispheric PLV study of visuospatial attention,[42] we chose F7 to T3, F8 to T4, F7 to TP7, F8 to TP8, F7 to T5, F8 to T6, FT7 to T3, FT8 to T4, FT7 to TP7, FT8 to TP8, FT7 to T5, FT7 to T6 to represent the VAN pathway; and F3 to C3, F4 to C4, F3 to CP3, F4 to CP4, F3 to P3, F4 to P4, FC3 to C3, FC4 to C4, FC3 to CP3, FC4 to CP4, FC3 to P3, FC4 to P4 to represent the DAN pathway. In addition, the frequency of interest was restricted to that identified in the previous time–frequency analysis studies.

Statistical Analyses. Statistical analyses were conducted using SPSS version 20. Behavioral data were analyzed by a two-factorial repeated measure ANOVA with stimulus size (5°, 20°, 30°) with ocular dominance (dominant eye, nondominant eye) as the within-subject factor.

We first explored whether the oscillatory activity could discriminate the target and the standard condition across sixty eyes using normalized oscillatory power as a measure. To this end, we submitted the normalized power to a three-factorial repeated-measures ANOVA with factors stimulus condition (target vs. standard stimuli), ROI (frontal area, parietal area, ventral frontal area, and temporal area), and hemisphere (left, right).

We next subdivided the data according to ocular dominance and compared dominant vs. nondominant eyes to explore the specific stimulus size-related attentional differences for each. We conducted a three-way ANOVA with factors ocular dominance (dominant eye, nondominant eye), ROI (frontal area, parietal area, ventral frontal area, and temporal area), and hemisphere (left, right) for the normalized power for each stimulus size. To further test the ability to distinguish the distinct stimulus sizes, the normalized power was used as the dependent variables, and stimulus size (5°, 20°, 30°), ROI (frontal area, parietal area, ventral frontal area, and temporal area) and hemisphere (left, right) as the within-subject factors in the two ocular dominance conditions, respectively. Further analysis was carried out with pair-wise comparisons, ANOVA and post hoc comparisons to calculate interaction effects.

The reliability of the functional connectivity was first performed by a paired t-test between the baseline PLV (the mean of the PLV from –500 ms to –200 ms) and the post-target PLV (the mean of the PLV from 50 ms to 250 ms), computed with α set to less than 0.05. To compare the PLV among different conditions, standardized PLV (SPLV) for each time point was computed using a z-transform normalization: post-stimulus PLV (the PLV from 50 ms to 250 ms) minus mean of the baseline PLV (the PLV from –500 ms to –200 ms), divided by the SD of the baseline PLV. The SPLV between each area was performed by a two-way ANOVA with factors stimulus size (5°, 20°, 30°), ocular dominance (dominant eye, nondominant eye) as the within-subject factor. Bonferroni corrections were used to correct multiple comparisons of areas.

For all ANOVAs, a P value of less than 0.05 was considered significant and Greenhouse–Geisser corrections were applied when sphericity was violated and effect sizes were calculated using partial eta squared (partial η^2). All pairwise comparisons were adjusted via Bonferroni corrections and the adjusted P value was reported. Tukey's HSD test was used for post hoc analyses.

A post hoc power analysis for ANOVA using GPower version 3.1.9.7.[43] was performed to evaluate whether the results had sufficient verification power. Only the results with statistical power over sufficient limits (80%) were statistically effective.[44] The relevant statistical power and effect sizes of the results are listed in Supplementary Table S1.

Correlation Analyses. We further used a relative measure [Ln (x2/x1)][45] to calculate the percent differences between the two eyes. Here, x2 represented dominant eye condition, and x1 represented nondominant eye condition, which showed the percentage increase or decrease of the corresponding index (performance, or EEG measures) in the dominant eye compared with that in the nondominant eye condition.

Spearman's Rho correlation coefficient analyses were used to evaluate the correlation of the percent difference of behavioral performance with the percent difference of EEG measures including event-related oscillation and connectivity indices. Only EEG signals for the target trials with correct responses were used in these analyses. This nonparametric correlation method was used because the data are non-normally distributed and may contain outliers.

Results

Behavioral Results

Figure 3a shows the RT and accuracy rates for dominant and nondominant eye in 5°, 20°, and 30° stimulus conditions, respectively. The mean RT for the 5°, 20°, and 30° stimuli were 364 ms (SD = 5 ms), 386 ms (SD = 4 ms), and 394 ms (SD = 2 ms), with a significant main effect, F (2, 58) = 17.390, P = 0.000, partial η^2 = 0.375. Although the RT of the dominant eye was slightly shorter than that of the nondominant eye, there was no significant main effect of ocular dominance in the 5°, 20°, and 30° stimulus conditions. For detailed mean values and statistics, see Table 1.

The respective accuracy rates for the 5°, 20°, and 30° stimuli were 85.5% (SD = 0.9%), 77.6% (SD = 1.8%), 72.2%

Investigative Ophthalmology & Visual Science

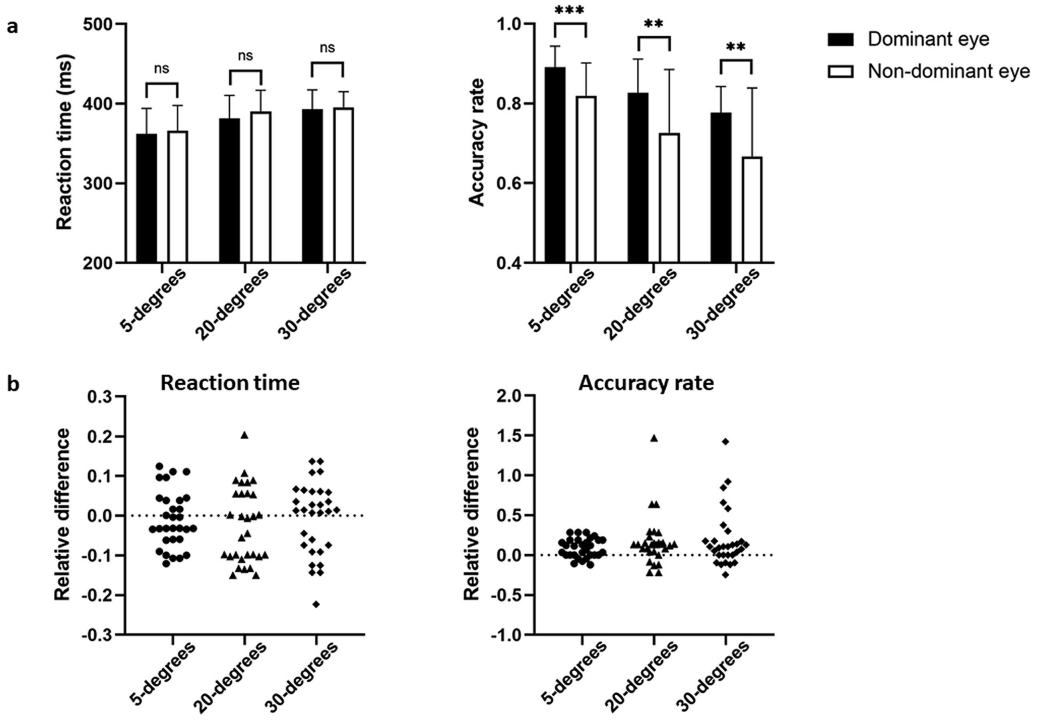

Figure 3. Behavioral differences between the dominant and nondominant eye. (**a**) A plot of an absolute measure of behavioral differences between the two eyes. Data are mean ± SD. The probability levels are $^{**}P < 0.01$, and $^{***}P < 0.001$. (**b**) A plot of a relative measure of differences between the two eyes. Circles indicate the 5° condition, triangles indicate the 20° condition, and squares indicate the 30° condition. The value of relative difference of greater than 0 indicate the percentage increase of behavioral performance in the dominant eye compared with that in the nondominant eye condition. The value of relative difference of less than 0 indicate the percentage decrease of behavioral performance in the dominant eye compared with that in the nondominant eye condition.

Table 1. The Mean Value and Comparisons of RT and Accuracy Rate at 5°, 20°, and 30° Stimuli Under the Dominant Eye and the Nondominant Eye Condition

Stimulus Size	Dominant Eye Condition	Nondominant Condition	F	*P* Value	Partial $\eta 2$
RT (ms)					
5° stimuli	362.22 (5.83)	365.95 (5.83)	0.623	0.436	0.021
20° stimuli	381.27 (5.31)	390.47 (4.83)	1.892	0.180	0.061
30° stimuli	393.07 (4.43)	395.45 (3.57)	0.133	0.718	0.005
Accuracy rate (%)					
5° stimuli	89.2 (1.0)	81.8 (1.5)	16.861	0.000	0.368
20° stimuli	82.7 (1.5)	72.6 (2.9)	10.981	0.002	0.275
30° stimuli	77.7 (1.2)	66.7 (3.1)	10.250	0.003	0.261

(SD = 1.6%), with a significant main effect, F (2, 58) = 25.845, $P = 0.000$, partial $\eta^2 = 0.471$. The accuracy rate of dominant eye was significantly higher than that of the nondominant eye in the 5°, 20° and 30° stimulus conditions. The detailed mean values and statistics were also presented in the Table 1.

Figure 3b showed the percent differences in RT and accuracy rate between the two eyes in 5°, 20°, and 30° stimulus conditions. There were more individuals showing the percentage increase of accuracy rate in the dominant eye compared with that in the nondominant eye condition. However, this condition was not noted for RT measurements.

Event-Related Oscillation Results

To explore the task dependency in the oddball task, we first compared the power of brain oscillations between the target and standard condition. The target and the standard condition in the oddball task differed in the phase-locked power in their theta, alpha and beta band (Fig. 4), but no significant differences were found in the total power and induced power, neither a main effect nor an interaction effect (n.s.). The mean phase-locked power of target stimuli was higher than the standard stimuli in all areas, and detailed statistics were presented in Supplementary Table S2.

Based on these results and previous studies,[46,47] we next explored the functional asymmetry between the dominant eye and the nondominant eye under the target condition. The main effects of ocular dominance were altered phase-locked power, while the total and induced power was not significant (n.s.).

Theta Band (4–7 Hz). Concerning the anterior area of VAN pathway, the phase-locked power revealed a significant difference between the dominant and nondominant eye

Investigative Ophthalmology & Visual Science

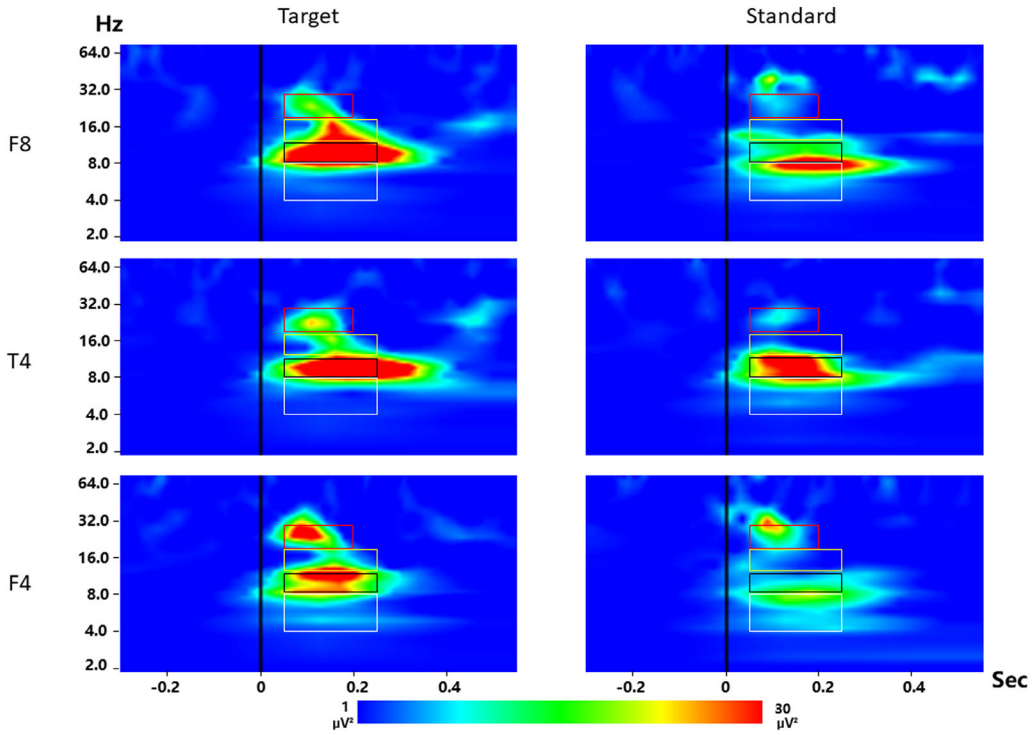

Figure 4. Target superiority of the phase-locked power in the theta, alpha band and beta sub-band over the right nodes of attention networks (F8, T4, F4). The power in the left hemisphere with the similar superiority effect was omitted in this part. Time frequency representations of phase-locked oscillatory power averaged across 5° (top panel), 20° (median panel) and 30° stimuli (bottom panel), plotted separately for the target (left panel) and the standard (right panel). The white, black, and yellow solid boxes indicated the theta (4–7 Hz), alpha (8–12 Hz), and low-beta (13–20 Hz) frequency band in the same time window (50–250 ms) of interest, respectively, that were averaged for the ANOVA. Meanwhile, the red solid boxes represented the high-beta (20–30 Hz) band in the time window (50–200 ms) of interest, which were also submitted to the ANOVA.

in the 5° stimulus condition (Fig. 5), F (1, 29) = 10.982, $P = 0.002$, partial $\eta^2 = 0.275$, and the mean power of the dominant eye condition (6.001 μV^2) was slightly higher than that in the nondominant eye condition (4.952 μV^2). In addition, in comparison with the nondominant eye, the dominant eye condition showed oscillatory power differences in the theta band over the anterior nodes of VAN as indicated by a respective change between the smaller central (5°, 20°) and the larger (30°) stimulus size (Fig. 5). There was a significant main effect of stimulus size in phase-locked power over the ventral frontal area, F (2, 58) = 12.786, $P = 0.000$, partial $\eta^2 = 0.306$. Meanwhile, the mean power of the 30° stimuli was lower than that of 5° ($P = 0.000$) and 20° stimuli ($P = 0.013$). However, there were no significant effects in the nondominant eye condition in any of the measures.

Concerning the posterior area of VAN pathway, both the dominant eye and the nondominant eye could transmit information that alters theta activity, showing a gradual change of neural activity towards the different stimulus sizes. For the dominant eye, the phase-locked power had a significant main effect of stimulus size, F (2, 58) = 14.634, $P = 0.000$, partial $\eta^2 = 0.335$; pair-wise comparisons showed that the mean power of 30° stimuli was smaller than the 5° ($P = 0.000$) and 20° stimuli ($P = 0.001$) with no interaction effect. For the nondominant eye, there was also a significant main effect of stimulus size, F (2, 58) = 8.549, $P = 0.001$, partial $\eta^2 = 0.228$, similar to those in the dominant eye condition. Furthermore, pair-wise comparisons revealed that with respect to 30° stimuli, both the power of 5° ($P = 0.004$) and 20° stimuli ($P = 0.003$) were slightly higher, respectively.

Concerning the DAN pathway, phase-locked power did not reveal significant differences between the dominant eye condition and the nondominant eye condition (n.s.).

Alpha Band (8–12 Hz). Considering that different frequency bands of alpha oscillation show a distinct type of task-related reactivity,[48] the present study further subdivided alpha oscillation into the low-alpha and high-alpha bands to separately analyze their functional roles.

Low-Alpha Band (8–10 Hz). For the anterior area of VAN pathway, there was a significant main effect of stimulus size in the dominant eye condition, F (2, 58) = 4.784, $P = 0.012$, partial $\eta^2 = 0.142$, and pair-wise comparisons indicated that the phase-locked power was significantly higher in the 5° than the 30° stimuli ($P = 0.010$). However, no such significant effects were observed in the nondominant condition.

For the posterior area of VAN pathway, the phase-locked power revealed a significant difference between the dominant and nondominant eye in the 20° stimulus condition (Fig. 6), F (1, 29) = 6.713, $P = 0.015$, partial $\eta^2 = 0.188$. And the mean power of the dominant eye condition (7.075 μV^2) was slightly lower than that in the nondominant eye condition (9.981 μV^2). In addition, the main effect analysis in the dominant eye condition showed that the low-alpha phase-locked power significantly depended on the stimulus size, F (2, 58) = 14.547, $P = 0.000$, partial $\eta^2 = 0.334$. Pair-wise

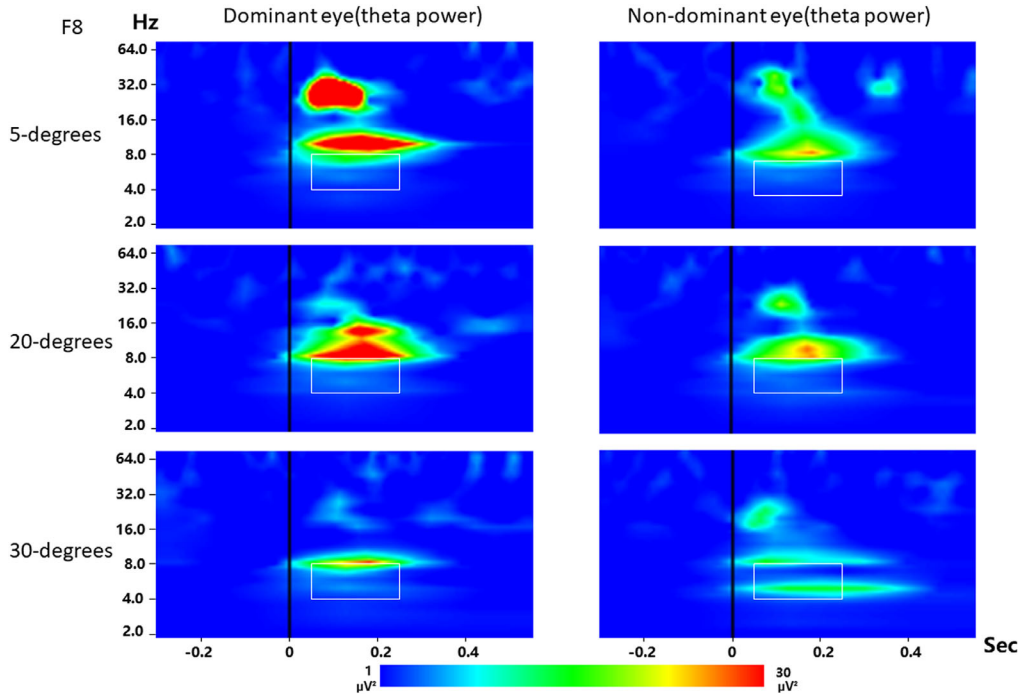

Figure 5. Visual cortical asymmetry of the theta phase-locked oscillatory power within the right ventral frontal area (F8) of VAN. The other theta activity within the nodes of VAN showing the similar trend was omitted. The time-frequency spectrogram of theta phase-locked power separately plotted for dominant eye (left panel) and nondominant eye (right panel) averaged across all trials within 5° (top panel), 20° (median panel) and 30° stimuli (bottom panel) blocks. The white rectangles indicated the theta (4–7 Hz) frequency band in the time window (50–250 ms) of interest, which were evaluated in the ANOVA.

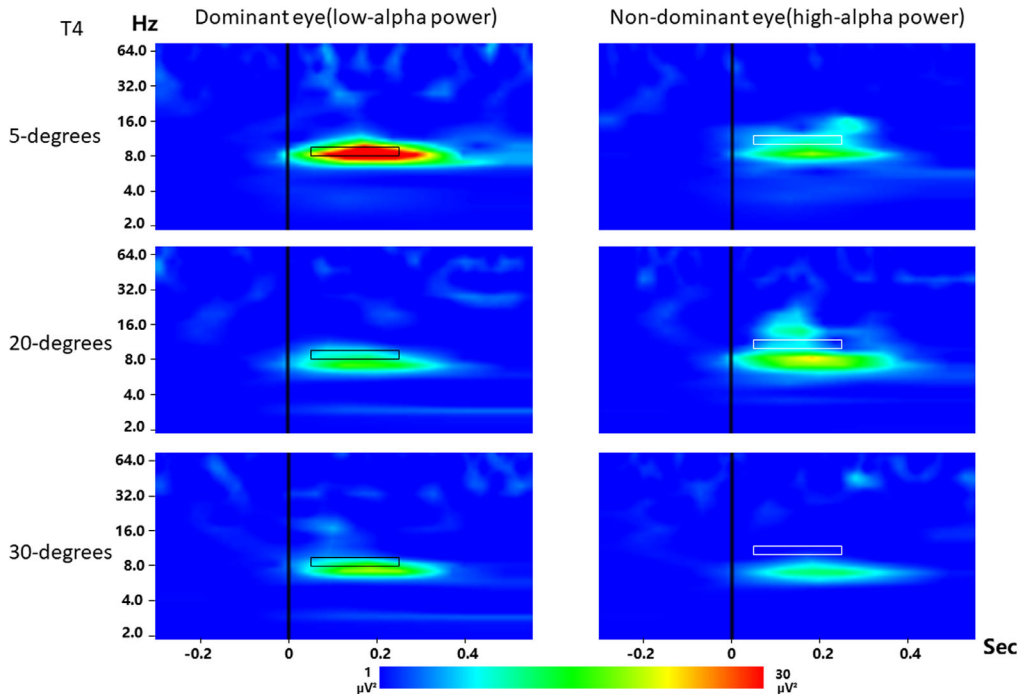

Figure 6. Visual cortical asymmetry of the low-alpha and high-alpha phase-locked oscillatory power within the right temporal area (T4) of VAN. The other alpha activity within the attention networks had been omitted. The time-frequency spectrogram of different alpha phase-locked power separately plotted for dominant eye (left panel) and nondominant eye (right panel) among the 5° (top panel), 20° (median panel) and 30° stimuli (bottom panel). The black and white solid rectangles marked indicated the low-alpha (8–10 Hz) and high-alpha (10–12 Hz) frequency band in the same time window (50–250 ms) of interest separately that were submitted to the ANOVA.

Investigative Ophthalmology & Visual Science

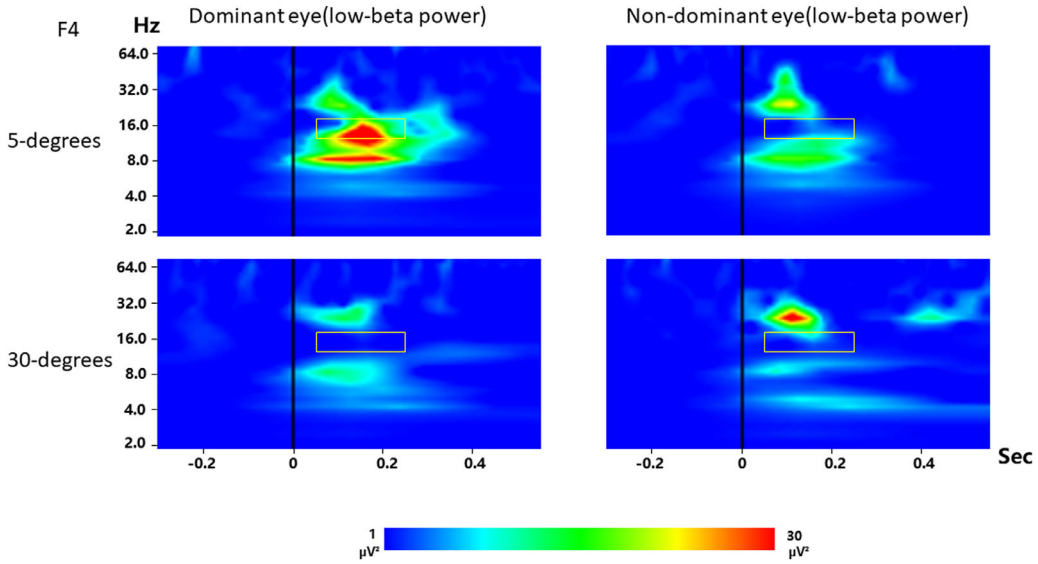

Figure 7. Visual cortical asymmetry of the low-beta phase-locked oscillatory power within the right frontal area (F4) of DAN in the specific stimulus sizes. The left part with the same asymmetric effect was omitted. Time frequency representations of phase-locked oscillatory power averaged across 5° (top panel) and 30° stimuli (bottom panel), plotted separately for dominant eye (left panel) and nondominant eye (right panel). The black rectangles indicated the time (50–250 ms) and frequency (13–20 Hz) of interest that were submitted to the ANOVA.

comparisons indicated that in comparison to the 5° stimuli (mean power: 12.482 μV^2), both the 20° (mean power: 7.075 μV^2) and the 30° stimuli (mean power: 5.961 μV^2) showed a strong power decrease ($P = 0.000$), although the low-alpha power in the nondominant eye condition had no such significant effects.

For the anterior area of DAN pathway, DAN analysis in ROIs found that significant differences between stimulus sizes in the dominant eye condition, F (2, 58) = 7.129, $P = 0.004$, partial $\eta^2 = 0.197$; pair-wise comparisons indicated that the phase-locked power of 30° stimuli was significantly lower than the 5° ($P = 0.003$) and 20° stimuli ($P = 0.014$), respectively. However, the low-alpha power over the anterior area of DAN in the nondominant eye condition showed no significant effects.

For the posterior area of DAN pathway, the dominant eye and nondominant eye condition showed no significant effects, neither a main nor an interaction effect (n.s.).

High-Alpha Band (10–12 Hz). Concerning the VAN areas, only the high-alpha oscillatory activity over the posterior area of VAN displayed significant effects of stimulus size. However, in contrast with the other frequency band oscillations, the dominant eye condition had no significant effect, whereas the nondominant eye condition did (Fig. 6). This difference was observed in the main effect of stimulus size, F (2, 58) = 4.068, $P = 0.040$, partial $\eta^2 = 0.123$, and in pair-wise comparisons between 5° and 30° stimuli ($P = 0.036$). In addition, pair-wise comparisons also indicated that the phase-locked power of 20° stimuli was significantly different from 30° stimuli ($P = 0.005$).

Concerning the DAN areas, the high-alpha phase-locked power showed no significant differences between the dominant eye and the nondominant eye condition (n.s.).

Beta Band (13–30 Hz). An effect was mainly found in the low-beta band; the high-beta oscillatory power did not show any significant effects. For the low-beta oscillatory activity (13–20 Hz), the significant difference between the dominant and nondominant eye condition was observed over the anterior area of both VAN and DAN, whereas the posterior areas had no significant differences.

For the anterior area of VAN, there was a significant main effect of ocular dominance in the 5° stimulus condition, F (1, 29) = 5.742, $P = 0.023$, partial $\eta^2 = 0.165$. Furthermore, the mean power of the dominant eye condition (5.358 μV^2) was higher than that in the nondominant eye condition (3.203 μV^2). In addition, the main effect of ocular dominance was also observed in the 30° stimulus condition, F (1, 29) = 5.019, $P = 0.033$, partial $\eta^2 = 0.148$. The mean power of the dominant eye condition (5.501 μV^2) was also higher than that in the nondominant eye condition (3.306 μV^2).

For the anterior area of DAN, there was a significant main effect of ocular dominance in the 5° stimulus condition (Fig. 7), F (1, 29) = 8.132, $P = 0.008$, partial $\eta^2 = 0.219$. The mean power of the dominant eye condition (4.101 μV^2) was slightly higher than that in the nondominant eye condition (2.979 μV^2).

PLV Results

There were no significant effects in beta band (n.s.), whereas the PLV over the theta, low-alpha, and high-alpha bands showed significant differences for the 5°, 20°, and 30° stimuli (Fig. 8).

Functional Connectivity in the Theta Band. Concerning the dominant eye, the PLV increased with increasing stimulus size. Specifically, there were significant theta PLV increases between the ventral frontal and the temporal area within the bilateral VAN in the 5° stimulus condition, t (29) = –4.659 for left VAN, $P < 0.001$; t (29) = –2.763 for right VAN, $P = 0.010$. In addition to the bilateral PLV enhancement between the nodes of VAN, t(29) = –2.768 for left VAN, $P = 0.010$; t(29) = –3.898 for right VAN, $P < 0.001$, there was a right PLV enhancement between the frontal and the parietal area within the DAN in the 20° stimulus condition, t(29) = –2.998 for right DAN, $P = 0.006$. In the 30° stimulus condition, we observed the bilateral PLV

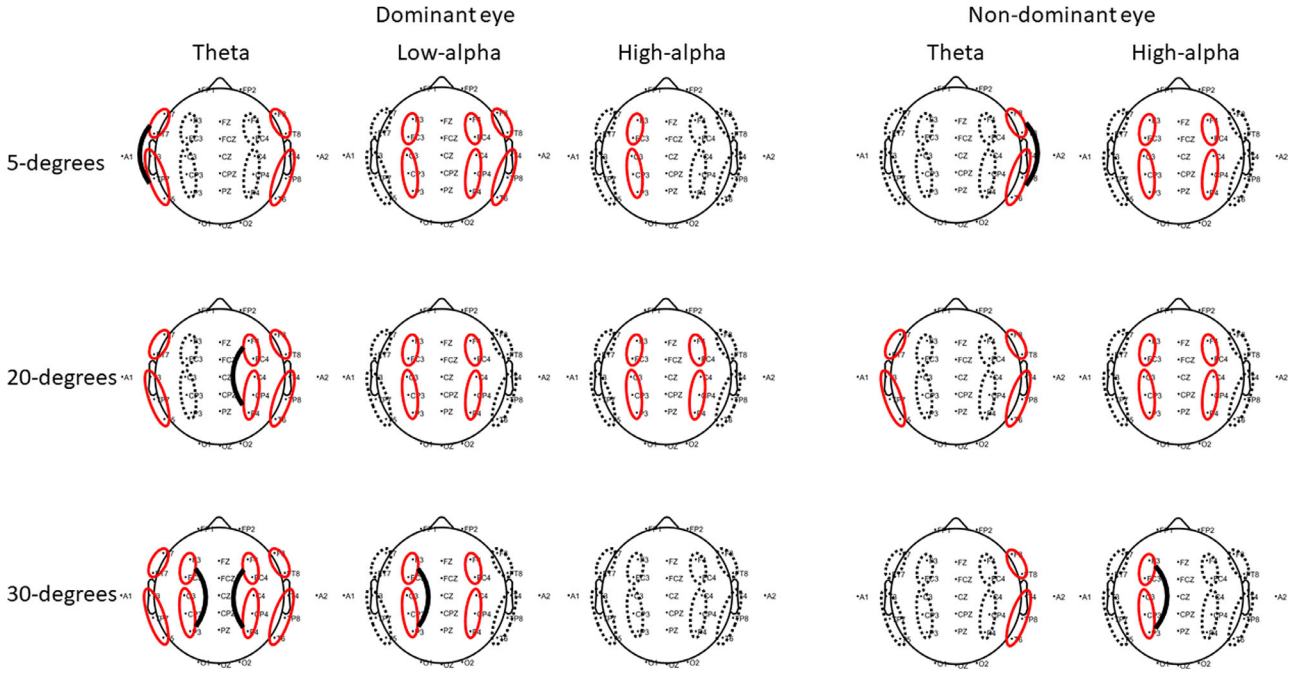

Figure 8. Increased phase synchronization over the theta, low-alpha and high-alpha band in the dominant eye (left panel) and in the nondominant eye (right panel). PLV averaged across all trials within 5° (top panel), 20° (median panel), and 30° stimuli (bottom panel) blocks. The ellipse represents the ROI within the DAN and VAN, which turned red if it was significant between baseline PLV and post-target PLV. The thick black line indicates the condition with a larger SPLV between the dominant eye and the nondominant eye.

enhancement between the nodes of VAN and DAN, t (29) = –2.283 for left VAN, $P = 0.030$; t (29) = –2.981 for right VAN, $P = 0.006$; t (29) = –3.082 for left DAN, $P = 0.004$; t (29) = –2.595 for right DAN, $P = 0.015$.

Meanwhile, the nondominant eye results showed that the VAN pathway had statistically significant theta PLV enhancement in the right hemisphere in all stimulus size conditions, t (29) = –3.375 for 5°, $P = 0.002$; t (29) = –3.995 for 20°, $P < 0.001$; t (29) = –2.578 for 30°, $P = 0.015$. But the phase synchronization in the left hemisphere of VAN was only observed in the 20° stimulus condition, t (29) = –3.989, $P < 0.001$.

We next wished to explore the attentional differences of the SPLV between the different ocular dominance conditions for specific stimulus condition. For the 5° stimulus condition, the SPLV of left VAN in the dominant eye condition was higher than that in the nondominant eye condition, mean values: 0.976, 0.339; F (1, 29) = 8.384, $P = 0.007$, partial $\eta^2 = 0.224$, whereas the SPLV of right VAN in the dominant eye condition was lower than that in the nondominant eye condition, mean values: 0.220, 0.769; F (1, 29) = 6.353, $P = 0.017$, partial $\eta^2 = 0.180$. Also, for this condition, the SPLV of the left DAN in the dominant eye condition was higher than that in the nondominant eye condition, mean values: 0.309, –0.040; F (1, 29) = 4.655, $P = 0.039$, partial $\eta^2 = 0.138$. For the 20° stimulus condition, the SPLV of the right DAN in the dominant eye condition was higher than that in the nondominant eye condition, mean values: 0.526, 0.020; F (1, 29) = 6.193, $P = 0.019$, partial $\eta^2 = 0.176$. For the 30° stimulus condition, both the left DAN, mean values: 0.523, 0.127; F (1, 29) = 4.701, $P = 0.038$, partial $\eta^2 = 0.139$, and the right DAN, mean values: 0.258, 0.119; F (1, 29) = 5.374, $P = 0.028$, partial $\eta^2 = 0.156$, showed the higher mean SPLV in the dominant eye condition than that in the nondominant eye condition.

Functional Connectivity in the Alpha Band.

Functional Connectivity in the Low-Alpha Band. With regard to the dominant eye, there was a right-lateralized PLV increase within the VAN in the 5° stimulus condition, t (29) = –2.322 for right VAN, $P = 0.027$. Besides, the bilateral low-alpha PLV enhancement between the frontal area and the parietal area of DAN exhibited statistically significant increases in all stimulus size conditions, 5°: t (29) = –3.888 for left DAN, $P = 0.001$; t (29) = –3.454 for right DAN, $P = 0.002$; 20°: t (29) = –2.688 for left DAN, $P = 0.012$; t (29) = –3.887 for right DAN, $P = 0.001$; 30°: t (29) = –3.397 for left DAN, $P = 0.002$; t (29) = –2.394 for right DAN, $P = 0.023$.

Meanwhile, the PLV results of nondominant eye revealed that neither the VAN pathway nor the DAN pathway had any statistically significant effects.

To test the effect further, we compared the SPLV between the dominant eye and the nondominant eye condition in specific stimulus conditions. There was a similar trend of the mean SPLV in all the VAN and DAN pathway, meaning that the dominant eye condition was higher than the nondominant eye condition. For detailed statistics, see Table 2.

Functional Connectivity in the High-Alpha Band. Contrary to the low-alpha band, there was greater high-alpha functional connectivity in the nondominant eye condition than in the dominant eye condition. Regarding the dominant eye, a significant PLV increase was observed between the frontal and the parietal area in the left hemisphere at the 5° stimulus condition, t (29) = –2.250 for left DAN, $P = 0.032$, whereas the high-alpha PLV increase

Table 2. The Mean (SD) Value and Comparisons of Low Alpha SPLV at 5°, 20°, and 30° Stimuli Under the Dominant Eye and the Nondominant Eye Conditions

Stimulus Size	Pathway	Dominant Eye Condition	Nondominant Condition	F	*P* Value	Partial $\eta 2$
5° stimuli	Left DAN	1.10 (0.17)	0.70 (0.24)	2.615	0.117	0.083
	Right DAN	1.11 (0.31)	0.71 (0.31)	0.898	0.351	0.030
	Left VAN	0.29 (0.26)	−0.73 (0.34)	5.100	0.032	0.150
	Right VAN	0.67 (0.27)	−0.25 (0.36)	3.289	0.080	0.102
20° stimuli	Left DAN	0.81 (0.25)	0.33 (0.32)	1.136	0.295	0.038
	Right DAN	0.47 (0.30)	0.36 (0.23)	0.072	0.790	0.002
	Left VAN	0.41 (0.31)	0.14 (0.24)	0.500	0.485	0.017
	Right VAN	0.18 (0.26)	−0.34 (0.30)	1.581	0.219	0.052
30° stimuli	Left DAN	1.38 (0.44)	0.09 (0.31)	4.472	0.043	0.134
	Right DAN	0.48 (0.34)	0.10 (0.57)	0.451	0.507	0.015
	Left VAN	−0.18 (0.34)	−0.28 (0.37)	0.031	0.863	0.001
	Right VAN	0.73 (0.27)	0.14 (0.43)	1.180	0.286	0.039

between the nodes of DAN exhibited bilateral enhancement in the 20° stimulus condition, t (29) = –2.675 for left DAN, $P = 0.012$; t (29) = –3.458 for right DAN, $P = 0.002$. No significant PLV enhancement of VAN was found in all conditions.

Specifically, in the nondominant eye, high-alpha PLV increase between the frontal area and the parietal area within the DAN appeared in the bilateral hemisphere at 5°, t (29) = –3.388 for left DAN, $P = 0.002$; t (29) = –3.159 for right DAN, $P = 0.004$, and 20°, t (29) = –2.899 for left DAN, $P = 0.007$; t (29) = –2.128 for right DAN, $P = 0.042$, stimulus conditions, whereas there was only left high–alpha PLV increase within the DAN in the 30° stimulus condition, t(29) = –3.147 for left DAN, $P = 0.004$. No significant PLV enhancement was observed in the VAN.

Further comparisons of the SPLV, for the 5° stimulus condition, the SPLV of the left VAN in the nondominant eye condition was lower than that in the dominant eye condition mean values: –1.103, –0.013; F (1, 29) = 9.023, $P = 0.005$, partial $\eta^2 = 0.237$. For the 20° stimulus condition, the SPLV of the left VAN in the nondominant eye condition was also lower than that in the dominant eye condition, mean values: –1.137, 0.330; F (1, 29) = 5.433, $P = 0.027$, partial $\eta^2 = 0.158$. For the 30° stimulus condition, the SPLV of the left DAN in the nondominant eye condition was higher than that in the dominant eye condition, mean values: 1.510, 0.206; F (1, 29) = 7.019, $P = 0.013$, partial $\eta^2 = 0.195$.

Correlation Analyses

Fig. 9 showed the significant correlations among the percent difference between the two eyes in RTs, accuracy rates, phase-locked power, functional connections. Further, Figure 10(a) and (b) showed the significant correlations of RT difference measure with neuronal differences. The percent difference of RT was positively correlated with the percent difference of low-alpha oscillations (Spearman $\rho = 0.276$, $P = 0.008$) and the percent difference of low-beta oscillations (Spearman $\rho = 0.223$, $P = 0.035$) in the posterior DAN area. Figure 10(c) and (d) showed the significant correlations of accuracy rate difference measure with neuronal differences. The percent difference of accuracy rate was positively correlated with the percent difference of low-alpha oscillations in the anterior DAN area (Spearman $\rho = 0.212$, $P = 0.045$) and the percent difference of low-alpha SPLV of left DAN (Spearman $\rho = 0.267$, $P = 0.035$).

Discussion

Using a tristimuli oddball task in combination with EEG recordings, we characterized the spatiotemporal oscillations and interareal communication in the brain which serve salience detection and the engagement of attention using stimuli with increasing levels of difficulty (stimulus sizes). This allowed us to probe possible differences between the dominant eye versus the nondominant eye. Behavioral results showed a delay in RTs and a decrease in accuracy rates as stimulus size increases to probe increasing difficulty of attention. RT of the dominant eyes tended to be faster, and accuracy rates significantly higher compared with nondominant eyes, confirming earlier observations.[19,49] Our EEG analyses revealed a complex pattern of frequency-specific responses and functional connectivity differences within the VAN and DAN, showing functional asymmetry between the dominant and nondominant eye. We now discuss these results and presumed information transmission pathways during the salience detection and attentional process in the dominant and nondominant eye, and the implications of these results (Fig. 11).

The phase-locked event-related oscillations revealed functional difference between the dominant and nondominant eyes and the association with certain frequency components at the different stimulus size levels. Concerning the theta rhythm, both the dominant and nondominant eye condition had a gradual change of theta activity appeared over the posterior area of VAN (i.e., temporal area), where it may serve a more general processing mechanism, such as visual information encoding, which requires the recruitment of the primary visual cortex (V1) modulated by visual attention after target presentation.[50] However, for the anterior area of VAN, the theta power of the dominant eye condition was larger than the nondominant eye condition for 5° stimuli. The greater theta power in the dominant eye indicates that there is more neural active engagement[51] and more long-range information transfer of synchronized neuronal activity across brain areas.[52] Thus, the theta power in the dominant eye may support the transfer of information to the frontal cortex to support its role in recognizing object representation (e.g. stimulus size, shape).[53]

To further study the functional asymmetry between the two eyes in the theta band by using functional connectivity, we found that both the dominant and nondominant eye had the VAN activations, which was in agreement with the above event-related oscillations results. However,

Investigative Ophthalmology & Visual Science

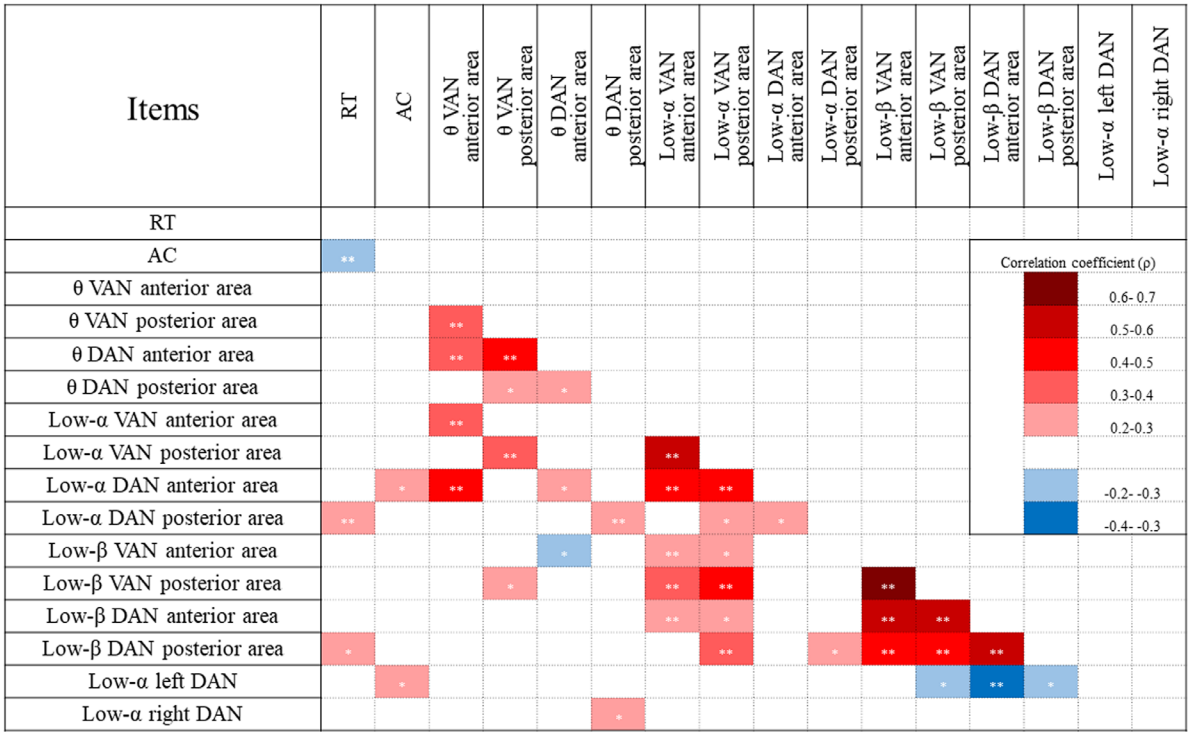

Figure 9. Correlations analysis between the percent difference in RTs, accuracy rates, phase-locked power, functional connections. The probability levels are **0.01, and *0.05 (2-tailed). Red color indicates the positive correlation between the two percent differences, whereas blue color indicates the negative correlation between the two percent differences. Items that were not statistically significant were omitted.

the dominant eye was activated bilaterally, whereas the nondominant eye was only activated in the right hemisphere under almost all the stimulus size conditions. Except for the above object recognition, the emergence of a theta-oscillation network reflects active neuronal processing for sustained attention.[54] We therefore proposed that visual information processed by the dominant and nondominant eye have different fates, that is, travelling different hemispheric VAN pathways, yet both together are supporting object recognition and sustained attention. In short, when visual signals reach the brain from the dominant eye and nondominant eye, theta activities may trigger initial network activations to encode visual attentional information, recognize object representation and maintain the current attention state.

To characterize the detailed relationships between alpha oscillations and visual attention processing, we divided the alpha band into the low-alpha and high-alpha band. The dominant eye condition showed significant low-alpha activity in the VAN areas and the frontal area of the DAN, whereas for the nondominant eye condition it did not. To our surprise, in contrast with the low-alpha oscillation of the dominant eye, the high-alpha local activity could only be found in the nondominant eye over the temporal area of VAN. This finding may reflect the sequential processing mechanism of the visual attention that the dominant eye with the low-alpha oscillation was more sensitive to the general cognitive demands such as the allocation of the attention resources during target processing. In contrast, the nondominant eye with the high-alpha oscillation was more closely linked to the anticipatory attention effect before the target detection.[55,56]

To further study the relationship between the sub-band of alpha oscillations and the ocular dominance, we analyzed the frequency-specific functional connections between the nodes of attention networks with diverse stimulus sizes. On the one hand, we found that all low-alpha functional connections of the dominant eye condition tended to be higher than the nondominant eye condition, which was basically consistent with the event-related oscillations results. During the attention allocation process for target processing, the dominant eye relied on low-alpha connections within the DAN to provide large scale integration across frontal and parietal regions, supporting a top-down modulation of bottom-up information.[57] In addition, as the task difficulty increases, the above low-alpha activities within DAN send top-down signals to suppress the bottom-up activation of the VAN,[58] which may explain the gradual disappearance of low-alpha VAN connectivity. That is to say, although the attention networks are supported by different structures in both hemispheres, the bottom-up and top-down dual modulatory mechanism of activities is closely intertwined during attention processing.[59]

In contrast, the high-alpha connectivity showed a prominent role in the nondominant eye, which was also consistent with the event-related oscillations results. This further confirmed the anticipatory function of high-alpha coherence because it increased during response preparation and execution.[60] And the high-alpha band synchronization connecting frontal and parietal regions thus supports the attentional top-down coordination mechanism to improve behavioral performance.[61] However, there were no significant correlations between the interareal communication and the behavioral performances, which might be related to the small sample size in the specific stimulus size presentations

Investigative Ophthalmology & Visual Science

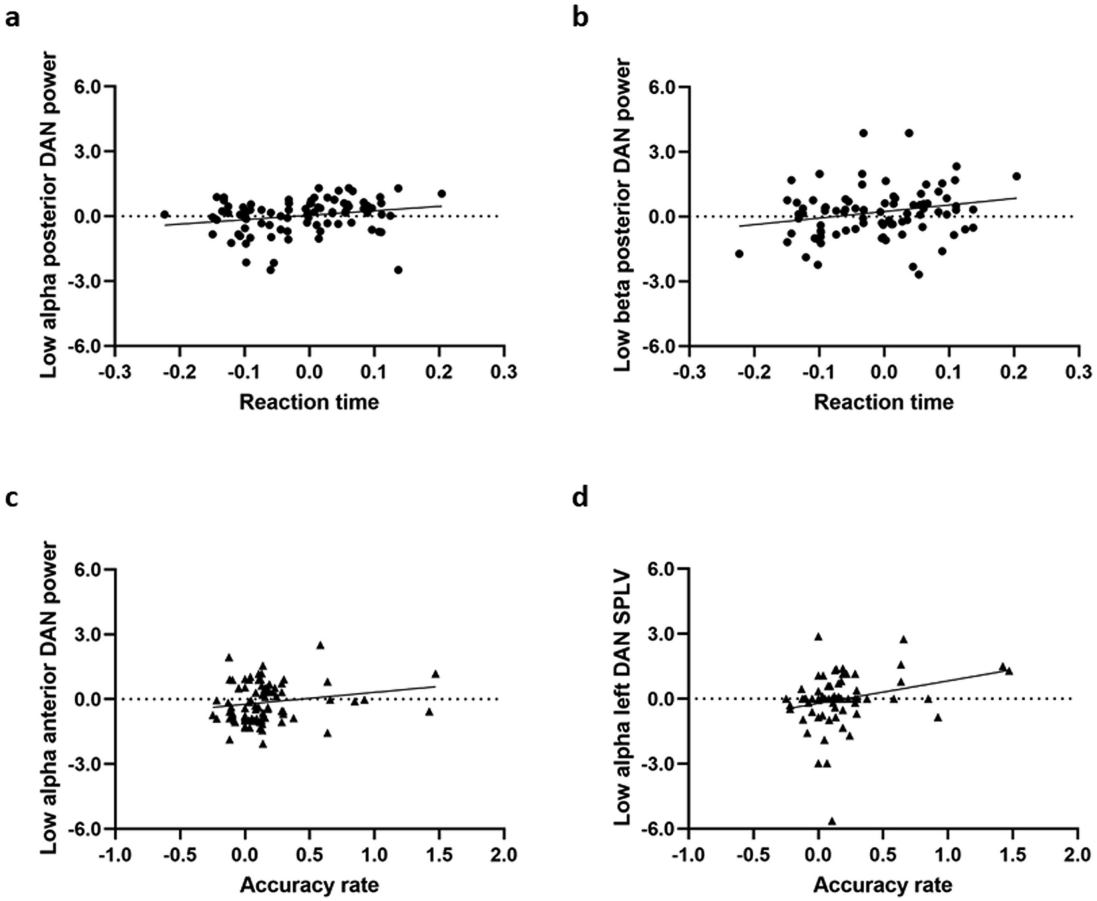

Figure 10. The correlation between behavioral differences and neuronal differences. (**a**) The correlation between the percent difference of RTs and the percent difference of low alpha in the posterior DAN area. (**b**) The correlation between the percent difference of RTs and the percent difference of low beta oscillations in the posterior DAN area. (**c**) The correlation between the percent difference of accuracy rate and the percent difference of low alpha oscillations in the anterior DAN area. (**d**) The correlation between the percent difference of accuracy rate and the percent difference of low alpha SPLV of left DAN.

when calculating functional connectivity; more evidence from future studies is necessary. To sum up the alpha band results, the dominant eye mainly relies on low-alpha rhythm within the different attention networks to process the attentional target stimuli and filter the unattended information, whereas the nondominant eye mainly relies on high-alpha rhythm within DAN to anticipatory attention.

In addition, the frontal area in both VAN and DAN pathway had the low-beta band differences between the dominant and nondominant eye condition in the 5° stimulus condition, whereas only the ventral frontal area had significant differences in the 30° stimulus condition. This beta power in the bilateral frontal area was higher for the dominant eye, suggesting an enhanced activation of attention through the suppression of attentional shifts from focused attention to involuntary attention.[62] The 5° stimulus condition recruited more frontal beta activities, which may be the reason why it was easier to activate and maintain attention.[63] In sum, our suggestion is that the dominant eye provides a basis for attention activation and maintenance by triggering frontal beta activities, which was related to the inhibition of the attentional shift.

Given that participants made button responses in our task, here we discussed the effect of pressing the button on the oscillations and activity pattern. In this context, we have to discuss an uncommon mu rhythm. The mu rhythm occurs infrequently and only as a subset of the low-alpha band. It fluctuates near 10 Hz, which is called the alpha–mu rhythm.[64] Our correlation results revealed that the difference in accuracy rate between the two eyes was related to the low-alpha oscillations in the anterior DAN area and low-alpha connectivity of the left DAN. In our experiment, the low-alpha activity exhibited this 10 Hz mu rhythm, which was consistent with other studies showing higher mu frequency connections between frontal and parietal regions for subjects with higher accuracy of task.[65] The mu rhythm as an entrainment/gating mechanism represents an important information transformation function that connects perception and execution.[66] We speculate that target stimuli induced mu rhythm to generate motor planning and expectation when these stimuli were instructed to react by button response.[67] In addition, aiming to explore the characteristics of the different superiority with eyes in the condition of the homogeneous handedness, we have balanced the sample between the right and left eye, which may ascertain the advantage of having the same hemispheric control of their habitual hand during attention processing.[68] Therefore, the fact that all individuals are right-handed may not

Investigative Ophthalmology & Visual Science

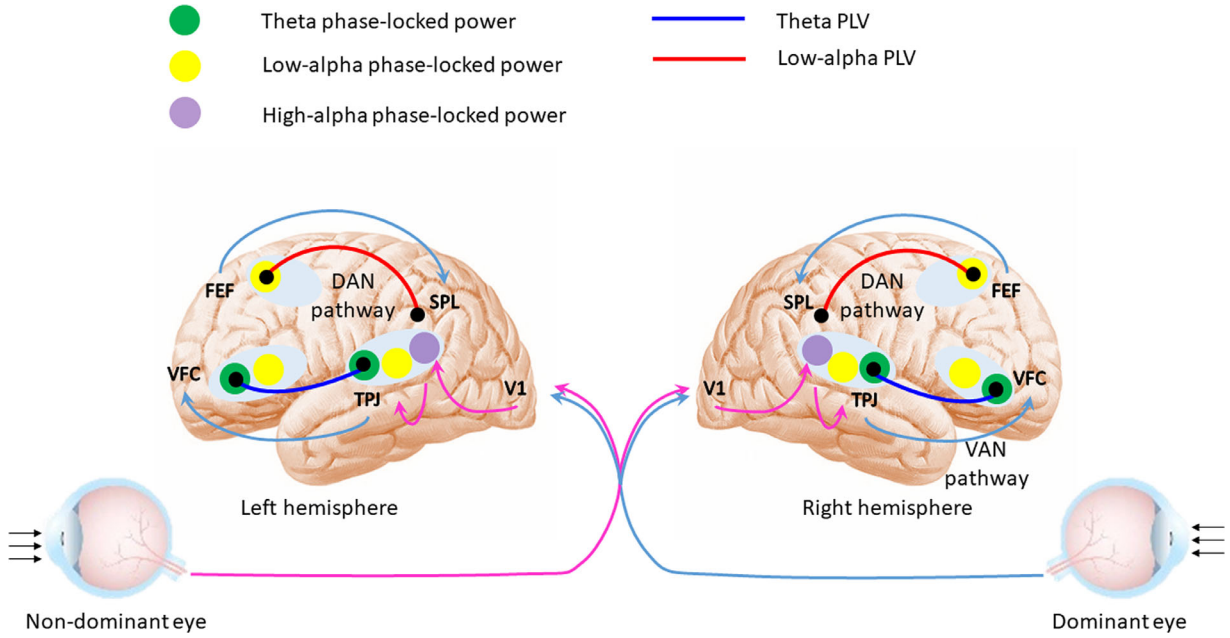

Figure 11. Schematic illustration of event-related oscillations, interareal communication and presumed information transmission pathways during the visual information processing. The grey ellipse denotes the nodes of attention networks and the green, yellow and purple circles represent the significant theta, low-alpha and high-alpha oscillatory activity among the distinct stimulus sizes, respectively. The black small circles reflect the electrodes that we used in functional connectivity. The dark blue and red line represents the theta PLV and the low-alpha PLV, respectively. Light blue and pink arrows indicate the possible direction of information transmission, which serve the dominant eye and nondominant eye separately during the visual information processing. FEF, frontal eye fields; SPL, superior parietal lobules; VFC, ventral frontal cortex; TPJ, temporoparietal junction.

affect the functional asymmetry of dominant and nondominant eyes to an unacceptable extent. However, the recruitment of left-handed individuals in future studies would help explore the relationships between manual preference and eye preference in attention networks.

There are also some shortcomings of our experiment. For instance, we did not study the influence of the subjects' ages. Especially, in childhood, the timing and duration of the visual experience (critical period) influences early neural development as it can alter the underlying neural networks. At an extreme, if vision is impaired in one eye, the cortex reorganizes to devote most of its workspace to the open eye.[53] Yet, the shift in ocular dominance in adults is slower and smaller and may use mechanisms distinct from those available to juveniles. The possible role of altered experience in early development in altering the underlying neural networks can be different in adulthood, which is an interesting question to be addressed in future research. In addition, the valuable findings were drawn out using such anatomic ROIs defined in normally sighted individuals in our study. However, considering a population where plasticity would have induced cortical reorganization during development, the reconstructive regions relevant to the visual attention networks may need carefully assessed in exploring the ocular dominance in this case. Furthermore, to better translate these findings into clinical practice, we should study patients with peripheral visual field defects as the experimental control in the future and combine our studies with functional magnetic resonance imaging. Because attention plays a great role in enhancement of residual vision,[69,70] future studies should explore the role of ocular dominance and functional asymmetry in affecting residual vision in patients with visual field defects.

Conclusions

Our study can be summarized as follows: during visual processing, the dominant and nondominant eyes can play different roles to ensure that tasks of different levels of difficulty can be completed. Specifically, when visual information reaches the eye, the brain areas within the nodes of DAN mainly driven by the nondominant eye applies the high-alpha activities to anticipate the upcoming stimulus before target detection. Thereafter, the brain areas within the nodes of VAN driven by both dominant and nondominant eye applies the theta-triggered initial network activities to encode visual attentional information to facilitate object recognition. Meanwhile, the brain processing of visual input from the dominant eye involves the attentional processing of specific features of the target stimuli which filters unattended information. The dominant eye thus provides a basis for attention activation and maintenance by triggering frontal beta activities to inhibit attentional shift. Besides, the dominant eye relies on the coupled low-alpha activities to recruit a bottom-up and top-down dual modulatory mechanism of the attention-related target detection and can process the different task difficulties through different information transmission streams of the attention networks (Fig. 11).

In conclusion, eye dominance can be explained by central brain processing and the EEG is a useful tool to help understand its physiological basis in normal visual and attention processing; and it has important implications for the diagnosis of visual system disorders and for finding means for early diagnosis, characterizing progression, or modulating it for recovery, restoration and rehabilitation through brain plasticity.

Investigative Ophthalmology & Visual Science

Acknowledgments

Supported by Grants 81871536 and 81971800 from the National Natural Science Foundation of China. We also appreciated the support from the Priority Academic Program Development of Jiangsu Higher Education Institutes (PAPD), China.

Author contributions: T.L. and C.X. conceived and designed this research. L.S. and Z.B. carried out the experiment. L.S. and S.C. analyzed and interpreted the data. M.X. prepared the figures. L.S., Z.B., B.S. T.L., and C.X. wrote the manuscript article. All authors reviewed the manuscript.

Disclosure: **S. Liu**, None; **B. Zhao**, None; **C. Shi**, None; **X. Ma**, None; **B.A. Sabel**, None; **X. Chen**, None; **L. Tao**, None

References

1. Kim H. Involvement of the dorsal and ventral attention networks in oddball stimulus processing: a meta-analysis. *Hum Brain Mapp*. 2014;35(5):2265–2284.
2. Zuo F, Panda P, Kotiuga M, et al. Habituation based synaptic plasticity and organismic learning in a quantum perovskite. *Nat Commun*. 2017;8(1):240.
3. Corbetta M, Shulman GL. Control of goal-directed and stimulus-driven attention in the brain. *Nat Rev Neurosci*. 2002;3(3):201–215.
4. Daitch AL, Sharma M, Roland JL, et al. Frequency-specific mechanism links human brain networks for spatial attention. *Proc Natl Acad Sci USA*. 2013;110(48):19585–19590.
5. Engel AK, Fries P. Beta-band oscillations–signalling the status quo? *Curr Opin Neurobiol*. 2010;20(2):156–165.
6. Capotosto P, Baldassarre A, Sestieri C, et al. Task and regions specific top-down modulation of alpha rhythms in parietal cortex. *Cereb Cortex*. 2017;27(10):4815–4822.
7. Kizuk SAD, Mathewson KE. Power and phase of alpha oscillations reveal an interaction between spatial and temporal visual attention. *J Cognitive Neurosci*. 2017;29(3):480–494.
8. Keil J, Pomper U, Senkowski D. Distinct patterns of local oscillatory activity and functional connectivity underlie intersensory attention and temporal prediction. *Cortex*. 2016;74:277–288.
9. Garcia-Rill E, D'Onofrio S, Luster B, et al. The 10 Hz frequency: a fulcrum for transitional brain states. *Transl Brain Rhythm*. 2016;1(1):7–13.
10. Yin S, Liu Y, Ding M. Amplitude of sensorimotor mu rhythm is correlated with BOLD from multiple brain regions: a simultaneous EEG-fMRI study. *Front Hum Neurosci*. 2016;10:364.
11. Coren S, Kaplan CP. Patterns of ocular dominance. *Am J Optom Arch Am Acad Optom*. 1973;50(4):283–292.
12. Mapp AP, Ono H, Barbeito R. What does the dominant eye dominate? A brief and somewhat contentious review. *Percept Psychophys*. 2003;65(2):310–317.
13. Ooi TL, He ZJ. Sensory eye dominance: relationship between eye and brain. *Eye Brain*. 2020;12:25–31.
14. Yang E, Blake R, McDonald JN. A new interocular suppression technique for measuring sensory eye dominance. *Invest Ophthalmol Vis Sci*. 2010;51(1):588–593.
15. Choi JA, Kim JS, Jeong HJ, et al. Ocular dominance is associated with the ganglion cell-inner plexiform layer thickness profile in the macula. *PloS One*. 2016;11(2):e150035.
16. Gimenez-Amaya JM. [Functional anatomy of the cerebral cortex implicated in visual processing]. *Rev Neurol*. 2000;30(7):656–662.
17. Jensen BH, Hougaard A, Amin FM, et al. Structural asymmetry of cortical visual areas is related to ocular dominance. *Neuroreport*. 2015;26(17):1071–1076.
18. Rombouts SA, Barkhof F, Sprenger M, et al. The functional basis of ocular dominance: functional MRI (fMRI) findings. *Neurosci Lett*. 1996;221(1):1–4.
19. Minucci PK, Connors MM. Reaction time under three viewing conditions: binocular, dominant eye, and nondominant eye. *J Exp Psychol*. 1964;67:268–275.
20. Momeni-Moghaddam H, McAlinden C, Azimi A, et al. Comparing accommodative function between the dominant and non-dominant eye. *Graefes Arch Clin Exp Ophthalmol*. 2014;252(3):509–514.
21. Nguyen KT, Liang WK, Muggleton NG, et al. Human visual steady-state responses to amplitude-modulated flicker: latency measurement. *J Vis*. 2019;19(14):14.
22. Li M, Liu X, Li Q, et al. The magnitude of the central visual field could be detected by active middle-late processing of ERPs. *Brain Res*. 2016;1650:41–50.
23. Wassle H, Grunert U, Rohrenbeck J, Boycott BB. Retinal ganglion cell density and cortical magnification factor in the primate. *Vision Res*. 1990;30(11):1897–1911.
24. Fujimoto N, Adachi-Usami E, Yah LH. The influence of miosis on the central visual field. *Nippon Ganka Gakkai Zasshi*. 1990;94(12):1157–1161.
25. Velten IM, Korth M, Horn FK, Budde WM. Temporal contrast sensitivity with peripheral and central stimulation in glaucoma diagnosis. *Br J Ophthalmol*. 1999;83(2):199–205.
26. Lopes-Ferreira D, Neves H, Queiros A, et al. Ocular dominance and visual function testing. *Biomed Res Int*. 2013;2013:238943.
27. Shah CT, Nguyen EV, Hassan AS. Asymmetric eyebrow elevation and its association with ocular dominance. *Ophthalmic Plast Reconstr Surg*. 2012;28(1):50–53.
28. Rigoni D, Brass M, Roger C, et al. Top-down modulation of brain activity underlying intentional action and its relationship with awareness of intention: an ERP/Laplacian analysis. *Exp Brain Res*. 2013;229(3):347–357.
29. Mouraux A, Iannetti GD. Across-trial averaging of event-related EEG responses and beyond. *Magn Reson Imaging*. 2008;26(7):1041–1054.
30. Anderson KL, Ding M. Attentional modulation of the somatosensory mu rhythm. *Neuroscience*. 2011;180:165–180.
31. Klimesch W. EEG alpha and theta oscillations reflect cognitive and memory performance: a review and analysis. *Brain Res Brain Res Rev*. 1999;29(2-3):169–195.
32. Miraval FK, Shie VL, Morales-Quezada L, et al. A preliminary study on qEEG in burn patients with chronic pruritus. *Ann Rehabil Med*. 2017;41(4):693–700.
33. Herrmann CS, Rach S, Vosskuhl J, Struber D. Time-frequency analysis of event-related potentials: a brief tutorial. *Brain Topogr*. 2014;27(4):438–450.
34. Ligeza TS, Wyczesany M, Tymorek AD, Kaminski M. Interactions between the prefrontal cortex and attentional systems during volitional affective regulation: an effective connectivity reappraisal study. *Brain Topogr*. 2016;29(2):253–261.
35. Okamoto M, Dan H, Sakamoto K, et al. Three-dimensional probabilistic anatomical cranio-cerebral correlation via the international 10-20 system oriented for transcranial functional brain mapping. *Neuroimage*. 2004;21(1):99–111.
36. Niedermeyer E, Lopes Da Silva FH. *Electroencephalography: Basic Principles, Clinical Applications, and Related Fields* (fifth ed.). Philadelphia, Baltimore, New York, London, Buenos Aires, Hong Kong, Sydney, Tokyo: Lippincott Williams & Wilkins, 2005.
37. Delorme A, Makeig S. EEGLAB: an open source toolbox for analysis of single-trial EEG dynamics including independent component analysis. *J Neurosci Methods*. 2004;134(1):9–21.
38. Tenke CE, Kayser J, Manna CG, et al. Current source density measures of electroencephalographic alpha

predict antidepressant treatment response. *Biol Psychiatry*. 2011;70(4):388–394.
39. Lachaux JP, Rodriguez E, Martinerie J, Varela FJ. Measuring phase synchrony in brain signals. *Hum Brain Mapp*. 1999;8(4):194–208.
40. Wang BA, Viswanathan S, Abdollahi RO, et al. Frequency-specific modulation of connectivity in the ipsilateral sensorimotor cortex by different forms of movement initiation. *Neuroimage*. 2017;159:248–260.
41. Del RM, Greenlee MW, Volberg G. Neural dynamics of breaking continuous flash suppression. *Neuroimage*. 2018;176:277–289.
42. Doesburg SM, Green JJ, McDonald JJ, Ward LM. From local inhibition to long-range integration: a functional dissociation of alpha-band synchronization across cortical scales in visuospatial attention. *Brain Res*. 2009;1303:97–110.
43. Faul F, Erdfelder E, Lang AG, Buchner A. G*Power 3: a flexible statistical power analysis program for the social, behavioral, and biomedical sciences. *Behav Res Methods*. 2007;39(2):175–191.
44. Cohen J. *Statistical Power Analysis for the Behavioral Sciences*. 2nd ed.: Mahwah, NJ: Lawrence Erlbaum Associates, 1988.
45. Christian Graff. Expressing relative differences (in percent) by the difference of natural logarithms. *J Math Psychol*. 2014;60:82–85.
46. Harper J, Malone SM, Iacono WG. Theta- and delta-band EEG network dynamics during a novelty oddball task. *Psychophysiology*. 2017;54(11):1590–1605.
47. Jones R, Cleveland M, Uther M. State and trait neural correlates of the balance between work and nonwork roles. *Psychiatry Res Neuroimaging*. 2019;287:19–30.
48. Klimesch W, Sauseng P, Hanslmayr S. EEG alpha oscillations: the inhibition-timing hypothesis. *Brain Res Rev*. 2007;53(1):63–88.
49. Shneor E, Hochstein S. Eye dominance effects in feature search. *Vision Res*. 2006;46(25):4258–4269.
50. Fries P. Rhythms for cognition: communication through coherence. *Neuron*. 2015;88(1):220–235.
51. Ardid S, Vinck M, Kaping D, et al. Mapping of functionally characterized cell classes onto canonical circuit operations in primate prefrontal cortex. *J Neurosci*. 2015;35(7):2975–2991.
52. Wang XJ. Neurophysiological and computational principles of cortical rhythms in cognition. *Physiol Rev*. 2010;90(3):1195–1268.
53. Kandel E, Schwartz J. *Principles of Neural Science,* 5th ed. Upper Saddle River, NJ: McGraw-Hill Medical, 2013.
54. Clayton MS, Yeung N, Cohen KR. The roles of cortical oscillations in sustained attention. *Trends Cogn Sci*. 2015;19(4):188–195.
55. Capotosto P, Babiloni C, Romani GL, Corbetta M. Differential contribution of right and left parietal cortex to the control of spatial attention: a simultaneous EEG-rTMS study. *Cereb Cortex*. 2012;22(2):446–454.
56. ter Horst AC, van Lier R, Steenbergen B. Mental rotation strategies reflected in event-related (de)synchronization of alpha and mu power. *Psychophysiology*. 2013;50(9):858–863.
57. von Stein A, Sarnthein J. Different frequencies for different scales of cortical integration: from local gamma to long range alpha/theta synchronization. *Int J Psychophysiol*. 2000;38(3):301–313.
58. Blundon EG, Ward LM. Search asymmetry in a serial auditory task: neural source analyses of EEG implicate attention strategies. *Neuropsychologia*. 2019;134:107204.
59. Vossel S, Geng JJ, Fink GR. Dorsal and ventral attention systems: distinct neural circuits but collaborative roles. *Neuroscientist*. 2014;20(2):150–159.
60. Moore RA, Gale A, Morris PH, Forrester D. Alpha power and coherence primarily reflect neural activity related to stages of motor response during a continuous monitoring task. *Int J Psychophysiol*. 2008;69(2):79–89.
61. Lobier M, Palva JM, Palva S. High-alpha band synchronization across frontal, parietal and visual cortex mediates behavioral and neuronal effects of visuospatial attention. *Neuroimage*. 2018;165:222–237.
62. Fiebelkorn IC, Pinsk MA, Kastner S. A dynamic interplay within the frontoparietal network underlies rhythmic spatial attention. *Neuron*. 2018;99(4):842–853.
63. Gola M, Magnuski M, Szumska I, Wrobel A. EEG beta band activity is related to attention and attentional deficits in the visual performance of elderly subjects. *Int J Psychophysiol*. 2013;89(3):334–341.
64. Koshino Y, Isaki K. Familial occurrence of the mu rhythm. *Clin Electroencephalogr*. 1986;17(1):44–50.
65. van der Helden J, van Schie HT, Rombouts C. Observational learning of new movement sequences is reflected in frontoparietal coherence. *PloS One*. 2010;5(12):e14482.
66. Pineda JA. The functional significance of mu rhythms: translating "seeing" and "hearing" into "doing". *Brain Res Brain Res Rev*. 2005;50(1):57–68.
67. Llanos C, Rodriguez M, Rodriguez-Sabate C, et al. Mu-rhythm changes during the planning of motor and motor imagery actions. *Neuropsychologia*. 2013;51(6):1019–1026.
68. Serrien DJ, Ivry RB, Swinnen SP. Dynamics of hemispheric specialization and integration in the context of motor control. *Nat Rev Neurosci*. 2006;7(2):160–166.
69. Lu Q, Wang X, Li L, et al. Visual rehabilitation training alters attentional networks in hemianopia: an fMRI study. *Clin Neurophysiol*. 2018;129(9):1832–1841.
70. Poggel DA, Kasten E, Sabel BA. Attentional cueing improves vision restoration therapy in patients with visual field defects. *Neurology*. 2004;63(11):2069–2076.